

Optical Stark effects in the multiple exciton states at a stacking-fault plane in BiI_3 crystals

I. Akai, T. Karasawa, T. Komatsu, and Y. Kaifu

Department of Physics, Faculty of Science, Osaka City University, Sumiyoshi-ku, Osaka 558, Japan

(Received 1 October 1990)

We present the observation of an optical Stark effect on multiple exciton states localized at a stacking fault in layered crystal BiI_3 . The level anticrossings concerning the crystal ground state as well as the multiple exciton states are clearly seen in the wide range of excitation laser frequency from off to on resonance of the exciton states. This result is well described based on the dressed-multiple-exciton model. An additional spectral change is also discussed in connection with real exciton population.

The spectral properties of matter are modified by their dynamical coupling with a photon field. The induced level shift is known as the optical Stark effect (OSE), which has been extensively studied in atomic and molecular systems. Frölich, Nöthe, and Reimann succeeded in observing the spectral change of the $2p$ yellow-series exciton line in Cu_2O due to the OSE under the existence of an ir laser field tuned to the energy interval between the $1s$ and the $2p$ levels.¹ The first observation of dynamical coupling between an exciton state and the ground state (excitonic OSE) by a strong photon field was reported in semiconductor quantum-well structures.² Under the excitation below the intrinsic exciton resonance, the excitonic absorption peak shows an ultrafast blue shift accompanied by a bleaching,³ a result which has currently attracted attention from an optical device.³ The excitonic OSE is also an important theme as a fundamental problem of nonlinear optics in nonmetallic solids in which coherent excitation often plays an important role. The coherent strong-field phenomena of optically excited states in condensed matter are considerably different from corresponding ones in atomic systems, which has been investigated theoretically.^{4,5} However, the detailed observation of the excitonic OSE has not sufficiently been achieved in semiconductor crystals, because broad linewidths and overlapping of higher-energy states in typical exciton spectra make it hard to clarify the details of the OSE in solids.

In this Brief Report, we report on the OSE in a system consisting of multiple-exciton states localized at a stacking fault in layered BiI_3 crystals; they are called stacking fault excitons (SFE's).⁶ The main profiles of OSE can be described by the photon-dressed level model. Besides, the additional nonlinear effects concerning the virtual and real exciton population under the excitation by strong field are clearly resolved for the first time. The SFE's appear as a set of sharp absorption lines denoted by R , S , and T close to the bulk indirect exciton absorption edge as shown in Fig. 1(a). Although the absorption intensities of the R , S , and T lines depend on both the number and area of the stacking fault of each sample, they always appear at the same energy positions with the energy intervals of a few meV having almost constant intensity ratios

($R:S:T \sim 4:2:1$).⁶ The bulk exciton in BiI_3 has a strong Coulomb coupling resulting in a small exciton radius, and the wave function of relative motion is nearly confined within the unit cell. The electronic states have been well described by the cationic exciton model, in which lower-lying exciton states originate in the transition from $6s$ to $6p$ states in the Bi^{3+} cation.⁷ The SFE states can be derived from the lowest-lying bulk exciton states by the perturbation of the stacking fault. In BiI_3 crystals, a stack-

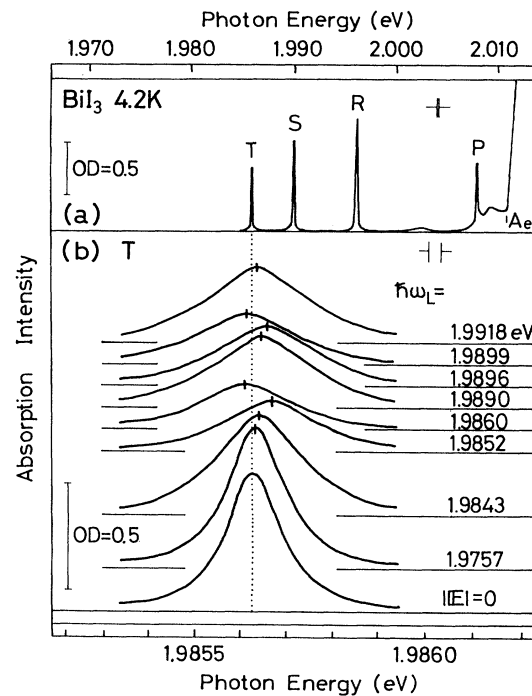


FIG. 1. (a) SFE absorption spectrum near the fundamental absorption edge in BiI_3 at 4.2 K. R , S , and T denote the absorption lines of SFE's; A_e , the absorption step due to the bulk indirect exciton transition (Ref. 6); P , the exciton transition due to a polytype effect (Ref. 14). (b) Absorption spectra of the lowest exciton T for several pumping-laser photon energies $\hbar\omega_L$ in enlarged scale; the lowest one is the absorption spectrum without laser excitation.

ing fault uniformly distorts the unit-cell symmetry in macroscopic area along the stacking fault plane and induces the energy localization and splitting from the bulk exciton states.⁷ Thus, the SFE's have rather large binding energies and large oscillator strengths compared to that of the direct bulk exciton transitions^{8,9} reflecting the characteristics of bulk exciton. The large binding energies isolate the exciton line spectra from the unbound electronic excitation region, which allows us to observe the excitonic OSE without worrying about free carrier effects when the pump-laser frequency is in the exciton region.

As seen in Fig. 1(a), the R , S , and T lines have extremely narrow linewidths without higher energy tails; that of T line in the sample used in this study is ~ 0.1 meV at 4.2 K. Furthermore, very sharp resonant luminescence lines appear without Stokes shift. A typical decay time constant on T luminescence is ~ 1 nsec.¹⁰ These facts verify that respective exciton-photon transformations occur directly at $\mathbf{k}=0$ and the indirect process is negligibly small.¹¹ In addition to these facts, the resonant luminescences of SFE extending over the exciting laser spot have been observed throughout the macroscopic area by space-resolved spectra.¹² This result shows the two-dimensional homogeneity of the stacking fault interface. Thus, the SFE states can be regarded as an ideal quasi-two-dimensional exciton system. Such characteristic spectral features of SFE's are favorable for us to study the coherent and incoherent excitation of exciton with intense photon field by the observation of fine OSE.

The exciton-exciton interaction of SFE has been observed under relatively low exciton density.^{11,13} In a previous paper, it has been suggested that the observed peak-energy shift for the off-resonance excitation would be related with an OSE.⁸ In the present study, we show detailed observation and analysis of the characteristic OSE in the system of multiple SFE states, where the spectral change of SFE is investigated in the wide excitation energy range of off- and on-resonance SFE states.

A dye laser (Rhodamin B) pumped by a pulsed N_2 laser was used for the pump beam. The laser beam was focused on the sample surface to less than 1 mm in diameter, which corresponds to the power density of $\sim 1.5 \times 10^5$ W/cm². The fluorescence from the dye cell was used for the probe light which has broad wavelength distribution covering the SFE transition region with the same time duration as the pump laser pulse of 7 nsec. The two beam paths were adjusted accurately to be coincident at the sample surface. The samples were immersed in a liquid-helium bath and the measurements were performed at 4.2 K.

On the same sample as for the absorption measurement presented in Fig. 1(a), the spectral change was measured under the pump laser excitation. The spectral change of the T line for various excitation laser photon energy $\hbar\omega_L$ is shown in Fig. 1(b) with enlarged photon energy scale. The lowest spectrum is the absorption spectrum without laser excitation ($E=0$), which coincides with that usually obtained. For lower energy excitation than T resonance $\hbar\omega_T (= 1.9856$ eV), the absorption peak shifts to blue. As $\hbar\omega_L$ approaches $\hbar\omega_T$, the blue shift becomes large and

the absorption intensity reduces. When $\hbar\omega_L$ increases beyond $\hbar\omega_T$, the peak shift changes from blue to red discontinuously. The same feature of spectral change on the T line was also observed at S resonance $\hbar\omega_S (= 1.9898$ eV) and R resonance $\hbar\omega_R (= 1.9950$ eV). The S and R lines exhibit similar $\hbar\omega_L$ dependence of spectral changes. Figures 2(a)–2(c) show the $\hbar\omega_L$ dependences of the peak shift values of the R , S , and T lines, respectively. The conspicuous features of observed results under the same exciting density are summarized as follows. (1) Resonant enhancement of the peak shift and the discontinuous peak-shift jump of the T line takes place for $\hbar\omega_L$ around and at all SFE resonances as shown in Figs. 1(b) and 2(c). Similar $\hbar\omega_L$ dependence of the peak shift on the R and S lines was also obtained as shown in Figs. 2(a) and 2(b), respectively. (2) The amount of peak-shift jump decidedly depends on the resonance energies; the large peak-shift jump occurs when the state itself is excited resonantly. As seen in the T line [Fig. 2(c)], the peak shift shows the largest jump for the resonant excitation at $\hbar\omega_T$. In the same manner, the large peak-shift jumps of the R and S lines appear at $\hbar\omega_R$ and $\hbar\omega_S$, respectively [Figs. 2(a) and 2(b)]. (3) In addition to such dispersionlike variation of peak shifts, a uniform peak shift in each line to the higher-energy side can be resolved about $\hbar\omega_T$. This additional blue shift becomes larger on the T , S , and R lines in order. (4) The absorption lines reduce their intensities remarkably for the excitation close to all resonances. The $\hbar\omega_L$ dependence of T absorption intensity is shown in Fig. 3, where the absorption intensity was normalized by that of the unperturbed one. The normalized intensity decreases to less than one half at each resonance energy.

The above results can be explained by the dressed-exciton model of a composite four-level system interacting with a monochromatic pump field of frequency ω_L . The four-level system consists of R , S , and T exciton states with $\mathbf{k}=0$ and the ground state. We consider two four-dimensional spaces. One is spanned by the product states of $\phi_\alpha = |\alpha, N-1\rangle$ and $\phi_G = |G, N\rangle$, α being R , S , and T exciton states, G being the ground state, and N indicating the number of photons of the pump-laser field. The other is spanned by $\psi_\alpha = |\alpha, N\rangle$ and $\psi_G = |G, N+1\rangle$. In the absence of the interaction, the state ψ_G (ϕ_G) is weakly degenerate or degenerate with one of the states ψ_α (ϕ_α); the energy levels are illustrated in Fig. 4(a). The eigensolutions of the exciton system combined with the photon field can be obtained by diagonalizing the four-dimensional Hamiltonian matrix for each space. By introducing the dipole interactions between each exciton and the ground state through the pump field as V_{RG} , V_{SG} , and V_{TG} , the matrix for the space $\{\psi_\alpha, \psi_G\}$ is written as

$$\begin{matrix} & \psi_R & \psi_S & \psi_T & \psi_G \\ \begin{matrix} \psi_R \\ \psi_S \\ \psi_T \\ \psi_G \end{matrix} & \left(\begin{array}{cccc} \hbar\omega_R & 0 & 0 & V_{RG} \\ 0 & \hbar\omega_S & 0 & V_{SG} \\ 0 & 0 & \hbar\omega_T & V_{TG} \\ V_{RG} & V_{SG} & V_{TG} & \hbar\omega_L \end{array} \right) & & & \end{matrix} . \quad (1)$$

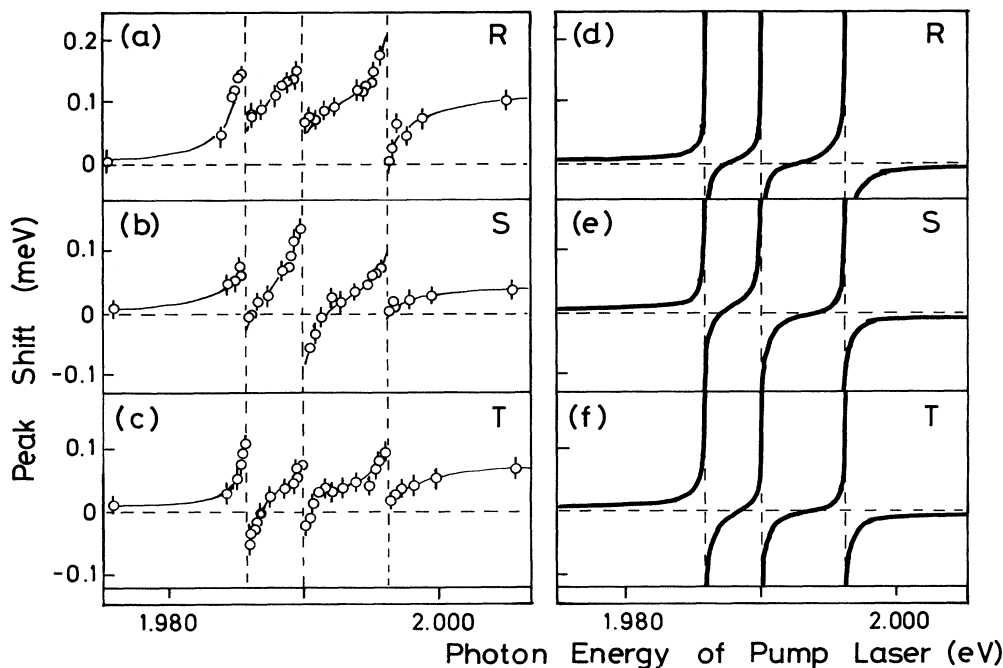


FIG. 2. (a)–(c) $\hbar\omega_L$ dependences of peak-shift values of the R, S, and T lines, respectively; vertical dashed lines: the resonance energies of the R, S, and T excitons, respectively. Thin solid lines are eye-guides only. (d)–(f) The model calculation of the $\hbar\omega_L$ dependences of peak-shift values by the dressed multiple exciton model. (See text.)

The Hamiltonian matrix for the space $\{\phi_\omega\phi_G\}$ is written in the same form, where the energies of diagonal components are shifted by the laser energy $\hbar\omega_L$. Neglecting the very small difference between $\sqrt{N+1}$ and \sqrt{N} for the strong field, we can assume that $V_{\alpha G}$'s are the same for both spaces. The energy levels of the dressed eigenstates Ψ_1 – Ψ_4 , and Φ_1 – Φ_4 are schematically shown in Fig. 4(b) as functions of $\hbar\omega_L$. Solid arrows in the figure indicate possible absorption processes of probe photons due to transitions from initial states Φ_4 and Φ_3 to final states Ψ_4 – Ψ_1 for $\hbar\omega_L$ around resonance of $\hbar\omega_T$. The energy shifts from the unperturbed states occur due to level anticrossings between mixed states. Thus, the peak shift

jumps from blue to red by turning the allowed transition components with changing $\hbar\omega_L$ beyond $\hbar\omega_T$. Then, for resonance excitation of $\hbar\omega_T$, the peak shift of the T line is caused by both of the anticrossings between final states

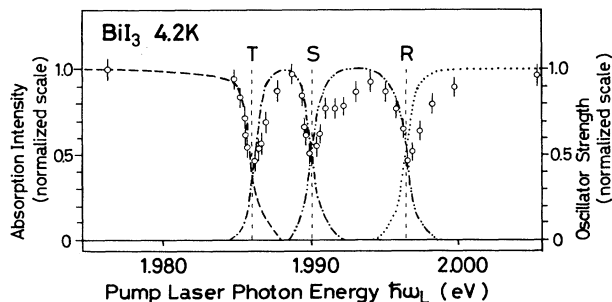


FIG. 3. Absorption intensity of the T line as a function of $\hbar\omega_L$. The intensity is normalized by that of the unperturbed T line. Four lines are the calculated oscillator strength f_{ij} of the T line, i and j denote the suffix of wave function Ψ_i and Φ_j , respectively, in Fig. 4(b). — — —, f_{34} ; - · - · -, f_{43} ; — · · —, f_{42} ; · · · · ·, f_{41} .

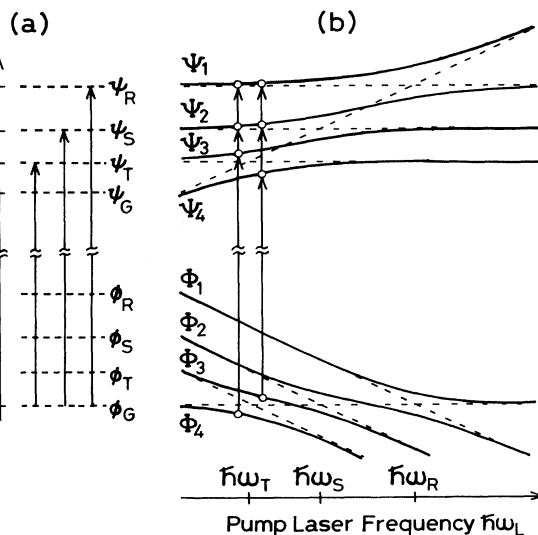


FIG. 4. (a) Energy diagram of the multiple-dressed-exciton states. ψ_R , ψ_S , ψ_T , and ψ_G : the SFE and the ground states with N photons; ϕ_R , ϕ_S , ϕ_T , and ϕ_G : the SFE states with $N-1$ photons and the ground state with $N+1$ photons, respectively. Upward arrows: the optical allowed exciton transitions. (b) Energy scheme of the multiple exciton model as a function of $\hbar\omega_L$. Ψ_i and Φ_j : the diagonalized final and initial states; upward arrows: the optical transitions between them.

and between initial states. On the other hand, only the initial-state anticrossing is responsible for the peak shifts of S and R lines under this excitation. This result implies that anticrossings of dressed exciton states and the ground state by a strong photon field are observed with clear separation for the first time. For higher energy excitations than S and R states, a similar situation occurs with changing $\hbar\omega_L$ beyond $\hbar\omega_S$ and $\hbar\omega_R$, and the same relation among the peak-shift jumps can be understood qualitatively along this line. As shown in Figs. 2(d)–2(f), the $\hbar\omega_L$ dependences of dispersionlike peak-shift values can be reproduced by a common parameter value of ~ 0.2 meV for V_{RG} , V_{SG} , and V_{TG} except for the uniform blue shift above $\hbar\omega_T$. This value gives a fairly large value of the dipole matrix element, which leads to a large optical nonlinear susceptibility $\chi^{(3)}$.

Using the obtained values of V_{RG} , V_{SG} , and V_{TG} , we calculate the $\hbar\omega_L$ dependence of the oscillator strength

$$f_{ij}(\hbar\omega_L) = |\langle \Psi_i(\hbar\omega_L) | \mathbf{P} | \Phi_j(\hbar\omega_L) \rangle|^2 \quad (i, j = 1, 2, 3, 4);$$

\mathbf{P} being the dipole moment. The result concerning the T exciton is shown by four kinds of lines in Fig. 3. The calculation well reproduces the experimental points for the excitation at the lower-energy side of each resonance. At the higher-energy side, the observed intensity reveals more reduction from the calculated ones.

Consequently, the dressed-multiple-exciton model well explains quantitatively the peak-shift jump and absorption reduction for each resonance. However, it is not valid for the additional blue shift and the larger amount of absorption reduction above resonance. These results must originate from the photocreated exciton population which is intrinsic in condensed matter contrary to the atomic system. Our laser power density, 1.5×10^5 W/cm², corresponds to the photon number 5×10^{15} cm⁻². The exciton density per unit volume could be roughly estimated to be at the most 10^{20} cm⁻³ from the values of exciton lifetime, the absorption intensity, and the effective thickness of the stacking fault plane. On the SFE system, the exciton density may be enough to give rise to the additional nonlinear effects by

high-density exciton population. Within our simple model, the absorption intensity should represent just the oscillator strength of the mixed product states. However, the population change in the eigenstates concerned seriously influences the absorption intensity. Among the four states Φ_3, Φ_4 and Ψ_3, Ψ_4 , for instance, higher-lying Ψ_3 or Φ_3 has more population under the excitation at the slightly higher side of T resonance, since it consists dominantly of the ground state ψ_G or ϕ_G . Then, the population relaxation from higher- (Ψ_3 or Φ_3) to lower-lying states (Ψ_4 or Φ_4) reduces the transition intensity. This is the case. Subsequently, the excessive absorption reduction may occur. Furthermore, by considering the fact that the additional blue shift appears even in the virtual excitation region at the slightly lower energy side of T , the light-induced renormalization of the exciton states caused by the virtual exciton creation⁴ must also be taken into account.

In this study, the optical nonlinear effects on the multiple SFE states induced by the virtual and real processes with the intense photon field have clearly been observed. The main part of the nonlinear effects by virtual excitation process can be quantitatively analyzed as an OSE by the multiple-dressed-exciton model. The additional blue shifts and the excessive absorption reduction can be understood from the viewpoint of photoinduced exciton population. For more detailed studies on the interaction between the photon field and exciton states in solids, the SFE's in BiI₃ should become a nice system, because the extremely narrow line shape and the large optical nonlinearity make it easy to observe spectral changes under the condition just below and above the resonance. Besides, multiple levels provide the situation of on resonance to one and off resonance to the other at the same time. From the experimental as well as theoretical aspects, further insights of time dependence on the optical nonlinear effect in this system are under investigation in the ultrafast time domain.

The authors wish to thank Professor T. Iida for stimulating discussions from a theoretical aspect.

¹D. Frölich, A. Nöthe, and K. Reimann, Phys. Rev. Lett. **55**, 1335 (1985).

²A. Mysyrowicz, D. Hulin, A. Antonetti, A. Migus, W. T. Masselink, and H. Morkoç, Phys. Rev. Lett. **56**, 2748 (1986); A. Von Lehmen, D. S. Chemla, J. E. Zucker, and J. P. Heritage, Opt. Lett. **11**, 609 (1986).

³B. Fluegel, N. Peyghambarian, G. Olbright, M. Lindberg, S. W. Koch, M. Joffre, D. Hulin, A. Migus, and A. Antonetti, Phys. Rev. Lett. **59**, 2588 (1987).

⁴S. Schmitt-Rink, D. S. Chemla, and H. Haug, Phys. Rev. B **37**, 941 (1988).

⁵S. Schmitt-Rink and D. S. Chemla, Phys. Rev. Lett. **57**, 2752 (1986); M. Combescot and R. Combescot, *ibid.* **61**, 117 (1988); R. Zimmermann, Phys. Status Solidi B **146**, 545 (1988); T. Higashimura, T. Iida, and T. Komatsu, *ibid.* **150**, 431 (1988).

⁶Y. Kaifu and T. Komatsu, J. Phys. Soc. Jpn. **40**, 1377 (1976).

⁷T. Komatsu, Y. Kaifu, S. Takeyama, and N. Miura, Phys. Rev. Lett. **58**, 2259 (1987).

⁸Y. Kaifu, J. Lumin. **42**, 61 (1988).

⁹T. Komatsu, Y. Kaifu, T. Karasawa, and T. Iida, Physica **99B**, 318 (1980).

¹⁰I. Akai, T. Karasawa, Y. Kaifu, A. Nakamura, M. Shimura, and M. Hirai, J. Lumin. **42**, 357 (1989).

¹¹K. Watanabe, T. Karasawa, T. Komatsu, and Y. Kaifu, J. Phys. Soc. Jpn. **55**, 897 (1986).

¹²T. Kawai, I. Akai, and T. Karasawa, J. Phys. Soc. Jpn. **58**, 969 (1989).

¹³S. Tatsumi, T. Karasawa, T. Komatsu, and Y. Kaifu, Solid State Commun. **54**, 587 (1985).

¹⁴T. Karawawa, T. Komatsu, and Y. Kaifu, Solid State Commun. **44**, 323 (1982).